Electronic Supplementary Material (ESI) for Journal of Materials Chemistry A.

Supporting Information

Efficiently Cogenerating Drinkable Water and Electricity from Seawater *via* Flexible MOFs Nanorod Arrays

*Xu Ma, Zhuoyi Li, Deng Zheng, Danke Chen, Xiaobin Wang, Xinyi Wan, Zhou Fang, Xinsheng Peng**

The file includes:

Video S1. The red LED is lighted up by device array under dark condition.

Video S2. The yellow LED is lighted up by device array under dark condition.

Video S3. The calculator is driven by device array under natural sunlight.

Video S4. The timer is driven by device array under natural sunlight.

Calculation of solar-vapor efficiency.

Detailed analysis of energy.

Additional Figures and Tables.

Calculation of solar-vapor efficiency.

The solar-vapor efficiency (η, %) of the PCG 2D SDIWE device is calculated using the following formula (2):

$$\eta = (\dot{m}h_{LV})/I \qquad (2)$$

where $\dot{m}$ is the mass flux of water evaporation, h_{LV} is the vaporization enthalpy, and I is the power density of 1 sun irradiation (1 kW m^{-2}). In PCG 2D SDIWE device, $\dot{m}$ is the average water evaporation rate under 1 sun is 1.51 kg m^{-2} h^{-1} based on Figure 3c, and h_{LV} is estimated to be about 1912 J g^{-1} based on the DSC measurement in the Figure S6. Therefore, the solar-vapor efficiency of the PCG 2D SDIWE device is 80.2%.

Detailed analysis of energy.

The consumption of input solar energy mainly includes: (i) solar reflection (3.5%), (ii) water evaporation (80.2%) and (iii) heat loss. The heat loss is mainly caused by radiation, convection and conduction.

(1) Radiation

The radiation heat loss of PCG 2D SDIWE device can be calculated by Stefan-Boltzmann Equation.

$$\varphi_{radd} = \varepsilon A\sigma\left(T_1^4 - T_2^4\right) \qquad (S1)$$

where φ_{radd} is heat radiation flux, ε is the emissivity of the PCG membrane, which is 0.965 in this work, A is the surface area of PCG membrane, σ is Stefan-Boltzmann constant (5.67×10^{-8} W m^{-2} K^{-4}), T_1 is the surface temperature of PCG membrane during evaporation (38.1 ℃) and T_2 is the ambient temperature (25.0 ℃). Therefore, the heat radiation loss is ~ 8.1% under 1 sun irradiation.

(2) Convection

The convection heat loss of PCG 2D SDIWE device can be calculated by Newton's law of cooling.

$$\varphi_{conv} = hA(T_1 - T_2) \quad \text{(S2)}$$

where φ_{conv} is heat convection flux, h is the convection heat transfer coefficient (5 W m^{-2} K^{-1}). T_1 is the surface temperature of PCG membrane during evaporation (38.1 ℃) and T_2 is the ambient temperature (25.0 ℃). Therefore, the convection heat loss is ~6.5% under 1 sun irradiation.

(3) Conduction

The conduction heat loss of PCG 2D SDIWE device can be calculated according to the following formula:

$$Q = Cm\Delta T \quad \text{(S3)}$$

where Q is conduction heat loss from PCG membrane to bulk water, C is specific heat of water (4.18 J g^{-1} K^{-1}), m is the weight of bulk water and ΔT is the elevated temperature of bulk water during evaporation. Due to water is transported from the bulk water to the membrane through the commercially available tissue, and the PCG membrane is placed on an insulating foam (the schematic illustration shown in Figure 3a, the PCG membrane and the foam are separated from the bulk water). The heat conduction from the PCG membrane to the bulk water is negligible, and there was no change in the temperature of bulk water ($\Delta T \approx 0$). Therefore, the conduction heat loss is ~ 0% under 1 sun irradiation.

Based on equation S1, S2 and S3, the heat loss of this PCG 2D SDIWE device is ~14.6%.

Additional Figures and Tables.

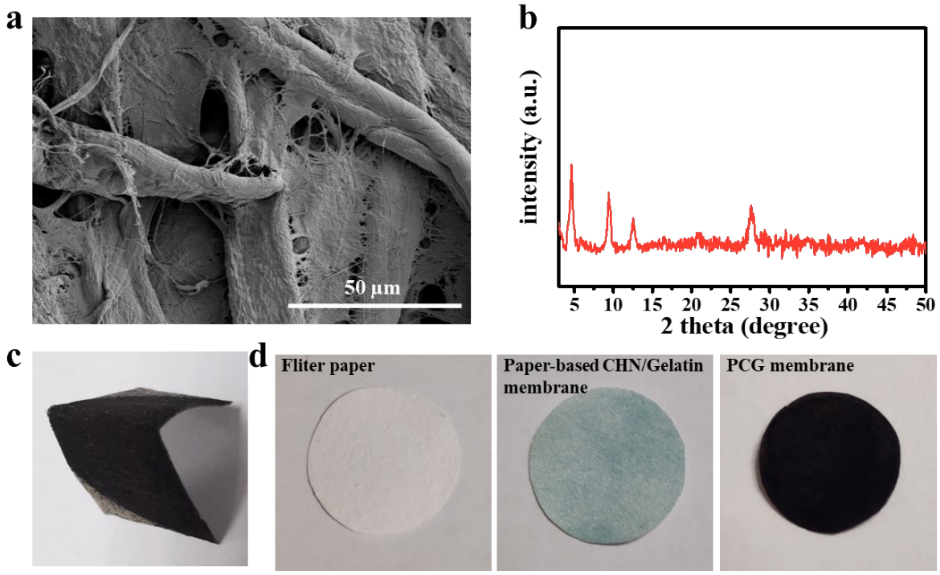

Figure S1 (a) SEM image of slow speed quantitative filter paper; (b) XRD pattern of Cu-CAT-1 MOF nanorod arrays; Photo images of (c) the folded PCG membrane; (d) filter paper, paper-based CHN/Gelatin membrane and PCG membrane, respectively.

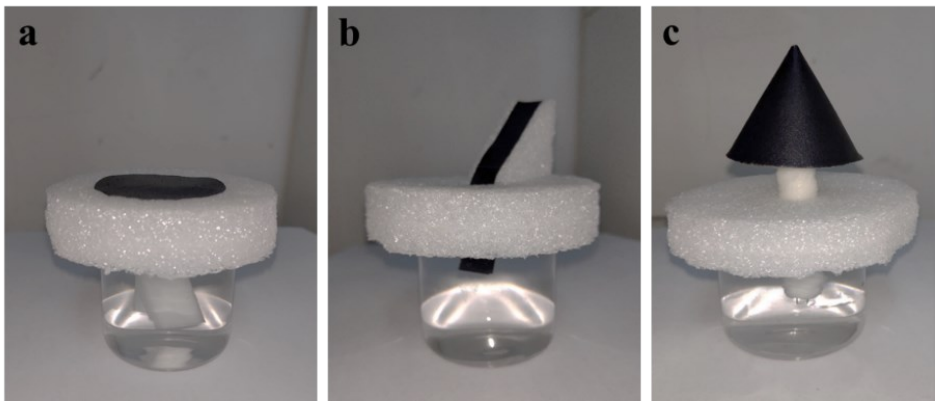

Figure S2. Digital images of the self-made water evaporation test device: (a) 2D SDIWE device; (b) 3D SDIWE device with 45º slope; (c) umbrella shaped 3D SDIWE device.

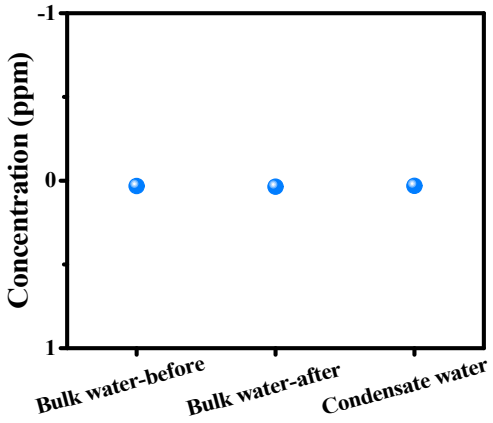

Figure S3. The concentrations of Cu^{2+} in condensate water and bulk water before and after the long-term evaporation experiment (12 hours).

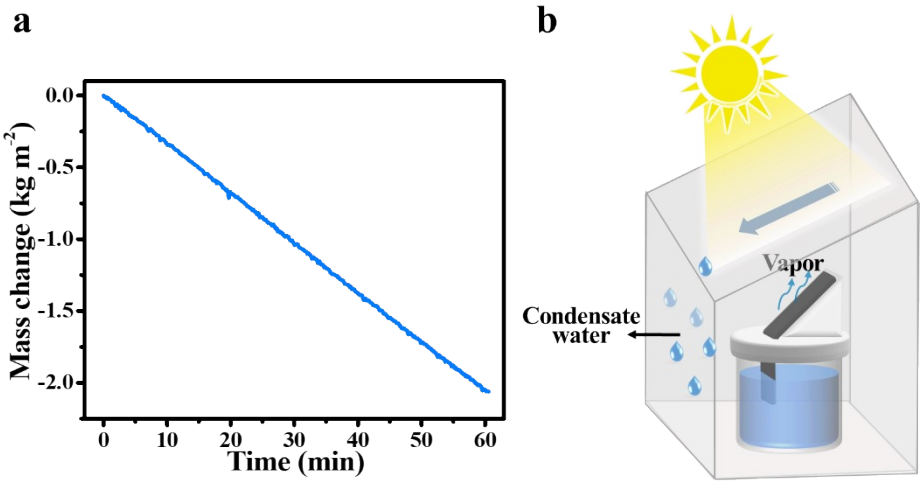

Figure S4. (a) Time-dependent mass change curve of 3D PCG SDIWE device with a slope of 45° using simulated seawater; (b) Schematic diagram of self-made water condensation device.

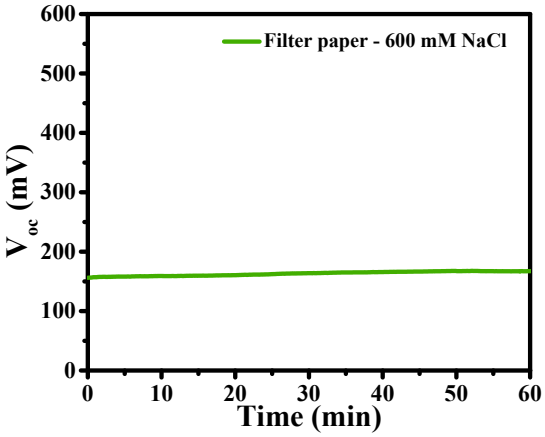

Figure S5. Time-dependent V_{oc} curve of filter paper in dark condition.

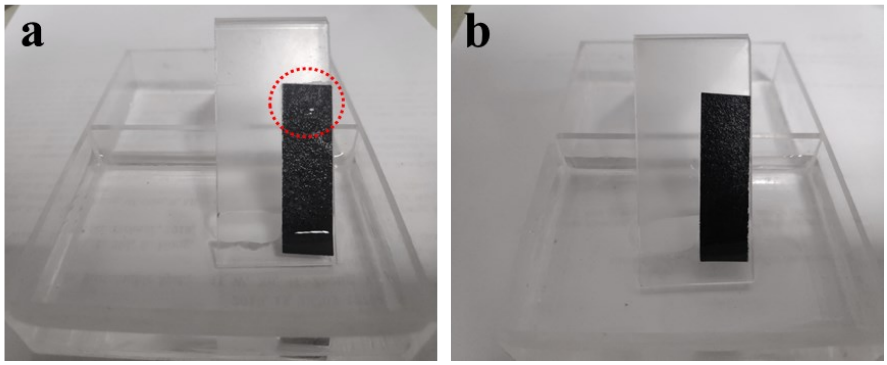

Figure S6. Digital images of (a) a small amount of salt precipitated on the surface of the ZSG membrane after 12 hours of solar irradiation; (b) the salt particles disappeared after 12 hours of standing at night.

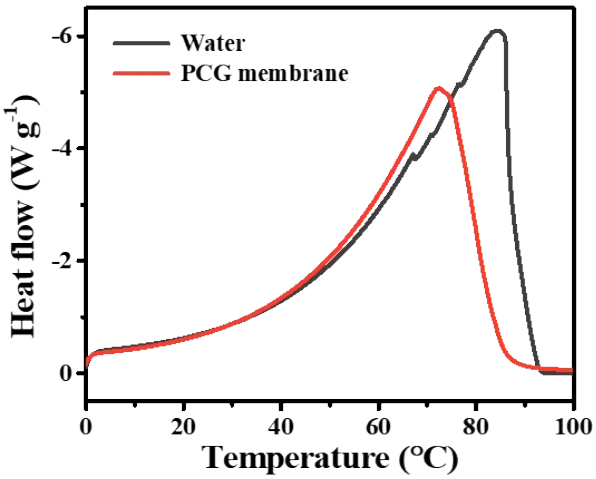

Figure S7. The the change of heat flow signal as a function of temperature.

Note: To obtain an accurate vaporization enthalpy of water in PCG membrane, the DSC measurement was conducted. During the vaporization enthalpy measurements, all of the samples were placed in an open Al crucible and heated with a linear heating rate of 5 ℃/min, under nitrogen flow flux (20 mL/min). Figure S6 shows the change of heat flow signal as a function of temperature. The measured enthalpy of water is 2283 J/g, which is very close to the theoretical value of 2257 J/g, indicating the accuracy of our measurements. Thus, the vaporization enthalpy of the water in PCG is 1912 J/g, which is smaller than that of pure water.

Table S1. Time-dependent temperature change of materials in dry state.

Materials	Time (s)	Temperature (℃)	Reference
Hierarchically nanostructured gel	50	~ 32	S1
Narrow-bandgap Ti_2O_3 nanoparticles	700	~52	S2
Multi-walled carbon nanotubes	10	45.5	S3
Dual-phase MoN/Mo_2N nanorambutans	10	83	S4
PCG membrane	10	52.6	This work

Table S2. The comparison of performance between PCG membrane and the references about solar desalination and evaporation induced electricity generation.

Materials	Solar vapor desalination	Evaporation induced electricity generation	Performances					Reference
			Evaporation rate (kg m^{-2} h^{-1})	Electricity output				
				V_{oc} (mV)	I_{sc} (μA)	Power density (mW m^{-2})	Electrolyte	
PCG membrane	✓	✓	2.07 (1 sun)	620	41	18.2	600 mM NaCl	This work
			natural evaporation under dark condition	558	32	12.8	600 mM NaCl	
CNTs/paper	✓	✓	1.15 (1 sun)	600	21	--	600 mM NaCl	S5
			natural evaporation under dark condition	470	7.5	--	600 mM NaCl	
GO/mixed cellulose ester films	✓	✓	1.3	310	5.3	--	pure water	S6
Graphene/carbon cloth	✓	✓	1.3	100	--	--	600 mM NaCl	S7
				370	--	--	500 mM NaCl	
Wet textile	✗	✓		200	80	--	100 mM NaCl	S8
AlOOH/UIO-66	✗	✓		30	--	--	100 mM KCl	S9
				1200	0.49	0.15	pure water	
Porous carbon film	✗	✓		40	--	--	100 mM NaCl	S10
				1000	1	0.6	pure water	
Carbon black	✗	✓		60	--	--	100 mM NaCl	S11
				1000	0.15	0.6	pure water	
Glass-fiber-carbon-nanoparticle film	✗	✓		5000	1.5	0.75	pure water	S12

Table 1 continued

Materials	Solar vapor desalination	Evaporation induced electricity generation	Performances					Reference
			Evaporation rate (kg m^{-2} h^{-1})	Electricity output				
				V_{oc} (mV)	I_{sc} (μA)	Power density (μW cm^{-2})	Electrolyte	
Ni–Al layered double hydroxide films	⚐	⚑		600	0.3	0.075	pure water	S13
Wood	⚐	⚑		300	10	0.3	pure water	S14
Al_2O_3 nanoparticles film	⚐	⚑		2500	0.8	0.07	pure water	S15
rGO sponges	⚐	⚑		630	110	17.4	pure water	S16
Carbon nanosphere@TiO_2 nanowires	⚐	⚑		1600	0.14	0.2	pure water	S17
GO/SA/CNT aerogels	⚑	⚐	1.622					S18
PVA/Ppy gels	⚑	⚐	3.2					S19
PVA/rGO hydrogel	⚑	⚐	2.5					S20
Carbonized mushroom	⚑	⚐	1.475					S21
MXene Ti_3C_2	⚑	⚐	1.33					S22
Vertically aligned graphene sheets membrane	⚑	⚐	1.62					S23
MOF-based hierarchical structure	⚑	⚐	1.5					S24
PPy-based cone	⚑	⚐	1.7					S25
ALD/Chinese ink with wood	⚑	⚐	1.31					S26
Paper-based rGO	⚑	⚐	1.778					S27

Note: '--' represents no mention in the references. Meanwhile, due to the lack of key parameters such as area, current, thickness, etc., we cannot calculate the corresponding area power density

References

[S1] F. Zhao, X. Zhou, Y. Shi, X. Qian, M. Alexander, X. Zhao, S. Mendez, R. Yang, L. Qu and G. Yu, *Nat. Nanotechnol.* **2018**, 13, 489-495.

[S1] J. Wang, Y. Li, L. Deng, N. Wei, Y. Weng, S. Dong, D. Qi, J. Qiu, X. Chen and T. Wu, *Adv. Mater.* **2017**, 29. 1603730.

[S3] X. Ma, Z. Deng, Z. Li, D. Chen, X. Wan, X. Wang and X. Peng, *J. Mater. Chem. A* **2020**, 8, 22728-22735.

[S4] L. Zhu, L. Sun, H. Zhang, D. F. Yu, H. Aslan, J. G. Zhao, Z. L. Li, M. Yu, F. Besenbacher and Y. Sun, *Nano Energy* **2019**, 57, 842-850.

[S5] P. Xiao, J. He, F. Ni, C. Zhang, Y. Liang, W. Zhou, J. Gu, J. Xia, S.-W. Kuo, T. Chen, *Nano Energy* **2020**, 68, 104385.

[S6] B. Hou, D. Kong, Z. Chen, Z. Shi, H. Cheng, D. D. Guo, X. Wang, *Appl. Therm. Eng.* **2019**, 163, 114322.

[S7] B. Hou, D. Kong, J. Qian, Y. Yu, Z. Cui, X. Liu, J. Wang, T. Mei, J. Li, X. Wang, *Carbon* **2018**, 140, 488.

[S8] S. S. Das, V. M. Pedireddi, A. Bandopadhyay, P. Saha, S. Chakraborty, *Nano Lett.* **2019**, 19, 7191.

[S9] Q. Ma, Q. He, P. Yin, H. Cheng, X. Cui, Q. Yun, H. Zhang, *Adv. Mater.* **2020**, DOI: 10.1002/adma.202003720e2003720.

[S10] T. Ding, K. Liu, J. Li, G. Xue, Q. Chen, L. Huang, B. Hu, J. Zhou, *Adv. Funct. Mater.* **2017**, 27, 22.

[S11] G. Xue, Y. Xu, T. Ding, J. Li, J. Yin, W. Fei, Y. Cao, J. Yu, L. Yuan, L. Gong, J. Chen, S. Deng, J. Zhou, W. Guo, *Nat. Nanotechnol.* **2017**, 12, 317.

[S12] J. Li, K. Liu, T. Ding, P. Yang, J. Duan, J. Zhou, *Nano Energy* **2019**, 58, 797.

[S13] J. Tian, Y. Zang, J. Sun, J. Qu, F. Gao, G. Liang, *Nano Energy* **2020**, 70, 104502.

[S14] X. Zhou, W. Zhang, C. Zhang, Y. Tan, J. Guo, Z. Sun, X. Deng, *ACS Appl. Mater. Interfaces* **2020**, 12, 11232.

[S15] C. Shao, B. Ji, T. Xu, J. Gao, X. Gao, Y. Xiao, Y. Zhao, N. Chen, L. Jiang, L. Qu, *ACS Appl. Mater. Interfaces* **2019**, 11, 30927.

[S16] G. Zhang, Z. Duan, X. Qi, Y. Xu, L. Li, W. Ma, H. Zhang, C. Liu, W. Yao, *Carbon* **2019**, 148, 1.

[S17] B. Ji, N. Chen, C. Shao, Q. Liu, J. Gao, T. Xu, H. Cheng, L. Qu, *J. Mater. Chem. A* **2019**, 7, 6766.

[S18] X. Hu, W. Xu, L. Zhou, Y. Tan, Y. Wang, S. Zhu, J. Zhu, *Adv. Mater* .**2017**, 29, 1604031.

[S19] F. Zhao, X. Zhou, Y. Shi, X. Qian, M. Alexander, X. Zhao, S. Mendez, R. Yang, L. Qu, G. Yu, *Nat. Nanotech.* **2018**, 13, 489.

[S20] F. Zhao, X. Zhou, Y. Shi, X. Qian, M. Alexander, X. Zhao, S. Mendez, R. Yang, L. Qu, G. Yu, *Nat. Nanotechnol.* **2018**, 13, 489.

[S21] N. Xu, X. Hu, W. Xu, X. Li, L. Zhou, S. Zhu, J. Zhu, *Adv. Mater.* **2017**, 29, 1606762.

[S22] R. Li, L. Zhang, L. Shi, P. Wang, *ACS Nano* **2017**, 11, 3752.

[S23] P. Zhang, J. Li, L. Lv, Y. Zhao, L. Qu, *ACS Nano* **2017**, 11, 5087.
[S24] Q. Ma, P. Yin, M. Zhao, Z. Luo, Y. Huang, Q. He, Y. Yu, Z. Liu, Z. Hu, B. Chen, H. Zhang, *Adv. Mater.* **2019**, 31, 17.
[S25] Y. Wang, C. Wang, X. Song, M. Huang, S. K. Megarajan, S. F. Shaukat, H. Jiang, *J. Mater. Chem. A* **2018**, 6, 9874.
[S26] H. C. Yang, Z. Chen, Y. Xie, J. Wang, J. W. Elam, W. Li, S. B. Darling, *Adv. Mater. Interfaces* **2018**, 6, 1.
[S27] Z. Wang, Q. Ye, X. Liang, J. Xu, C. Chang, C. Song, W. Shang, J. Wu, P. Tao, T. Deng, *J. Mater. Chem. A* **2017**, 5, 16359.